



Published in final edited form as:

*Spine (Phila Pa 1976)*. 2009 April 1; 34(7): 648–654. doi:10.1097/BRS.0b013e318197f013.

## Gait Abnormalities and Inflammatory Cytokines in an Autologous Nucleus Pulposus Model of Radiculopathy

Mohammed F. Shamji, M.D., Ph.D.<sup>1,2</sup>, Kyle D. Allen, Ph.D.<sup>1</sup>, Stephen So, B.S.<sup>1</sup>, Liufang Jing, M.Sc.<sup>1</sup>, Samuel B. Adams, M.D.<sup>1,3</sup>, Reinhard Schuh<sup>4</sup>, Janet Huebner, M.Sc.<sup>5</sup>, Virginia B. Kraus, M.D., Ph.D.<sup>5</sup>, Allan H. Friedman, M.D.<sup>6</sup>, Lori A. Setton, Ph.D.<sup>1,3</sup>, and William J. Richardson, M.D.<sup>3</sup>

<sup>1</sup>Department of Biomedical Engineering, Duke University, Durham, NC

<sup>2</sup>Division of Neurosurgery, The Ottawa Hospital, Ottawa, ON

<sup>3</sup>Division of Orthopedic Surgery, Duke University Medical Center, Durham, NC

<sup>4</sup>Gait Analysis Laboratory, Foot and Ankle Center, Vienna, Austria

<sup>5</sup>Department of Medicine, Duke University Medical Center, Durham, NC

<sup>6</sup>Division of Neurosurgery, Duke University Medical Center, Durham, NC

### Introduction

Intervertebral disc herniation can cause clinical radiculopathy based on mechanical deformation and biochemical irritation of apposed neural structures,<sup>1,2</sup> and subsequent clinical presentation vary greatly in the extent of pain, neurological deficit, and functional disability. A number of studies have applied autologous nucleus pulposus (NP) to the rat DRG as a model of non-compressive disc herniation, inducing inflammatory histopathology and neuronogial apoptosis, decreases in nerve conduction velocities, and onset of mechanical allodynia and thermal hyperalgesia.<sup>2–8</sup> A key mediator of these changes is suggested to be tumor necrosis factor alpha (TNF $\alpha$ ),<sup>9–11</sup> expressed at higher levels in herniated discs than degeneration-matched controls.<sup>12,13</sup> Furthermore, systemic immunomodulatory treatment targeting TNF $\alpha$  activity attenuates these effects in animal models<sup>14–17</sup> and may provide clinical relief of sciatica in human studies.<sup>18</sup> The impact of these changes on animal locomotor function remains questionable,<sup>5,19</sup> despite being of clinical interest.<sup>20</sup>

Involvement of TNF $\alpha$  in radiculopathy may relate to the presence of macrophages, more numerous and widespread than other inflammatory cells after herniation.<sup>21,22</sup> Recruitment of macrophages after disc herniation is incompletely understood, though it may relate to an underlying immune mechanism. The immune-privilege of the NP may lead to extracellular matrix or cellular structures recognition as antigenic upon systemic exposure following herniation, a theory supported by regional lymph node accumulation of lymphocytes after exposure to autologous NP,<sup>23</sup> and lymphocyte accumulation in the intervertebral disc after annular injury.<sup>24</sup> Further, IgM and IgG immunoglobulin deposition occurs in human herniated disc tissue, suggesting specific immune activation.<sup>25</sup> Given this antigenic potential of NP tissue, the immune response to herniated material may include cytokines involved in

Corresponding Author Mohammed F. Shamji M.D., M.Sc., Department of Biomedical Engineering, 136 Hudson Hall, Duke University, Durham, NC 27708, Phone: (919) 660-5453, Fax: (919) 681-8490, Email: E-mail: mohammed.shamji@duke.edu.

This project was approved by the Duke Institutional Animal Care and Use Committee (IACUC), protocol number A153-06-04.

lymphocyte differentiation and products of their activation. Markers of inflammatory and immune activation in this study are interleukins 23 (IL-23) and 17 (IL-17).

Lymphocyte transmigration occurs following peripheral nerve constriction injury, with efficient recruitment of CD4<sup>+</sup> lymphocytes and activation of local microglia to inflammatory phenotype.<sup>26</sup> Production of IL-23 preceded expression of IL-17 at the injury site, with the more important finding this IL-17 response was absent despite normal IL-23 levels in recombination-activating gene-1 knockout mice deficient in T-lymphocytes.<sup>27</sup> This supports the known role for T-lymphocytes producing IL-17; and indeed, IL-23 acts on naïve CD4<sup>+</sup> T-lymphocytes to facilitate differentiation and expansion into a Th17 lineage, characterized by substantial IL-17 production.<sup>28,29</sup> Further, there is evidence of a potential role of IL-23 and IL-17 in regulating an immune response in the peripheral nervous system. Glial cells also produce IL-23, with enhanced T-lymphocyte IL-17 release upon costimulation with a specific antigen, implicating the neuronal support cells with a role in immune activation.<sup>30,31</sup> Tissue effects of this mediator include blood-brain-barrier disruption with efficient lymphocyte transmigration<sup>32</sup> and further recruitment of CD4<sup>+</sup> lymphocytes and activation of local microglia to an inflammatory phenotype.<sup>26</sup>

This study evaluated an animal model of NP herniation radiculopathy for evidence of functional deficits of mechanical allodynia and altered gait patterns, and local expression of IL-23 and IL-17 for a role in the biochemical inflammatory process. The results demonstrate novel findings of gait asymmetry and imbalance between left and right duty factors, and confirm known findings of mechanical allodynia. Further, the results provide evidence of a role for both local inflammatory and immune activation, but not a systemic inflammatory response, after DRG exposure to autologous NP.

## Materials and Methods

### Surgical Induction of Radiculopathy

Male Sprague-Dawley rats (n=32, 9 months-old) were divided into Sham (n=16) and NP-treated (n=16) groups, and underwent surgery for NP removal and placement at a lumbar DRG in a procedure modified from that described previously,<sup>5,33,34</sup> and approved by Duke Institutional Animal Care and Use Committee (IACUC), protocol number A153-06-04.

Rats were anesthetized with intraperitoneal pentobarbital (40 mg/kg). A 1 cm incision was made on the dorsal surface of the proximal tail, followed by lateral retraction of traversing tendons to expose a caudal intervertebral disc. This disc was punctured and the NP was harvested into a curette. Single layer closure used 3-0 nylon sutures. Exposure of the right L5 DRG was accomplished by a midline dorsal incision, following which the thoracolumbar fascia was incised to the right of the L5 spinous process. Paraspinal muscle was retracted laterally exposing the facet joint and interlaminar space, followed by partial unilateral laminotomy and medial facetectomy revealing right L5 DRG. Sham animals were closed, while NP-treatment animals underwent placement of the autologous NP material onto the exposed DRG and were then closed. A two-layer closure used 3-0 vicryl sutures for fascia and 3-0 nylon sutures for skin. Animals were returned to solitary cage housing for 5–7 days, followed by group housing until sacrifice.

After evaluation of mechanical allodynia, thermal hyperalgesia, and gait (all described below), animals were sacrificed at designated time points (1, 2, 3, or 4 weeks after surgery, n=4 for each of sham and NP-treated groups) by intraperitoneal pentobarbital injection (60 mg/kg) after which blood was obtained via cardiac puncture for serum analysis of systemic cytokine levels. The exposed DRG was excised and placed in Optical Cutting Temperature (OCT) embedding media (Sakura Finetek, Torrance, CA) and frozen in liquid nitrogen.

## Evaluation of Mechanical and Thermal Sensitivity

Animals were evaluated for mechanical allodynia and thermal hyperalgesia pre-operatively and at post-operative time points. Mechanical sensitivity was tested by placing animals in a wire bottom cage and stimulating the ipsilateral (surgical exposure) or contralateral (no exposure) hindpaw with a 2g or 10g von Frey filament (Stoelting, Wood Dale, IL) normal to the plantar surface. Ten trials were performed at each force, and the number of paw withdrawals observed was recorded as a paw withdrawal frequency for each of the two filaments.

Thermal sensitivity was tested by focal limb stimulation (Hargreaves method)<sup>35</sup> and a tail-flick test. The animal was placed in an acrylic cage with a glass floor and a focused-light heat stimulus was applied separately to the ipsilateral or contralateral limb (IITC, San Diego, CA). Limb withdrawal latency was measured in 3 separate trials per limb, separated by five minutes. Rats were then placed in a disposable polyethylene restraint, and their unrestrained tail was placed beneath a focused light source. Tail withdrawal latency was measured in 3 separate trials per animal, separated by fifteen minutes. Heat application did not exceed 20 seconds in either experiment.

## Assessment of Animal Gait

Animal gait was determined pre-operatively and at post-operative time points. Locomotion was assessed by recording 4–7 gait trials (200 fps; Phantom V4.2, Vision Research, Wayne, NJ) in a custom-built, transparent arena with an underlying mirror oriented at 45°. The video frame (time) and geometric position of individual paws were marked at foot-strike and toe-off events using a custom designed subroutine (DLTdataviewer2) for MATLAB (Mathworks, Natick, MA). The derived gait parameters included: velocity (cm/sec), symmetry (time between left and right foot-strikes normalized by time between two left foot-strikes), stride frequency (foot-strikes/sec), duty factor (DF, time between foot-strike and toe-off events for a specific limb normalized by time between two foot-strike events for the same limb), stride length (cm), and step width (cm).

Given that acceleration affects these outcome variables, trials were screened for consistent velocity excluding those with fluctuations over 10% about the mean velocity. The difference between contralateral and ipsilateral limb duty factors was defined as  $\Delta DF$ . Thus, a positive  $\Delta DF$  indicates greater time spent on the contralateral limb, a negative  $\Delta DF$  indicates increased time spent on the ipsilateral limb, and  $\Delta DF$  statistically indistinct from 0 indicates no limb preference. Data from multiple strides were averaged, yielding per trial data.

## Quantification of Serum Cytokine Levels

The collected serum sample was processed for cytokine content of IL-1 $\alpha$ , IL-1 $\beta$ , IL-4, IL-6, IL-12, GM-CSF, IFN- $\gamma$ , and TNF $\alpha$  using a custom-designed cytokine multiplex bead assay kit (Invitrogen, Carlsbad, CA) and a Bio-Plex System plate reader (Bio-Rad, Hercules, CA).

## Dorsal Root Ganglion Immunohistochemistry

Frozen DRG blocks were cryosectioned (8  $\mu$ m), fixed in 4% formaldehyde (10 min, room temperature), and blocked for 30 min in 3.75% BSA (Invitrogen, Carlsbad, CA) and 5% goat serum (Invitrogen, Carlsbad, CA). Samples were then incubated with primary rabbit polyclonal anti-human IL-17 and IL-23 antibodies (sc-7927 and sc-50303, Santa Cruz Biotechnology, Santa Cruz, CA) diluted 1:33 in blocking solution for 60 min. Samples were washed in PBS and incubated with an AlexaFluor488 goat anti-rabbit secondary antibody (Invitrogen, Carlsbad, CA) diluted 1:100 in blocking buffer for 30 min. Cell nuclei were counterstained using 0.5 mg/mL propidium iodide (Sigma-Aldrich, St. Louis, MO) for 15 min and slides were mounted with GVA mounting solution (Invitrogen, Carlsbad, CA).

Samples were imaged using a confocal laser scanning microscope (Zeiss LSM 510, 63X water-immersion objective; Zeiss, Jena, Germany) identifying sections rich in ganglion cells, satellite cells, and Schwann cells. Three blinded graders independently evaluated sections for fluorescence staining uniformity and intensity using a semi-quantitative scale: 0 (no stain), 1 (moderate, non-uniform stain), 2 (moderate, uniform stain), 3 (intense stain) for each cell type. For each sample and cell type, an immunohistochemical score was averaged across all three graders to obtain a sample score.

### Statistical Analysis

Mechanical allodynia, thermal hyperalgesia, and gait data were analyzed by a full-factorial, generalized linear model (GLM) with treatment (NP-treatment or sham) as a factor and incorporating linear dependence on time. Stride length is linearly dependent on velocity, so the GLM to investigate stride length differences additionally included a linear dependence on velocity. When significance was observed, post-hoc Tukey's HSD tests were conducted to detect inter-group differences.

Serum cytokine levels and grade of immunohistochemical staining for each cell type and target were tested for evidence of differences across time and between sham and NP-treatment groups using two-factor multivariate analysis of variance (MANOVA) at the 0.05 level of significance. This allows evaluation of differences between multiple dependent variables without increasing the likelihood of Type I error. For immunohistochemical staining, interobserver reliability was evaluated across all cell types and targets, reported as a quadratic-weighted Kappa statistic.

## Results

### Mechanical Allodynia and Thermal Hyperalgesia

Animals in the NP-treatment group had increased mechanical sensitivity on the limb ipsilateral to surgical intervention as measured by the von Frey filament test for mechanical allodynia. Greater withdrawal frequencies were observed for the 10g filament among NP-treatment animals compared with sham animals (Figure 1,  $p < 0.02$ , GLM). These withdrawal frequencies were elevated above the pre-operative range for all time points in the NP-treatment group, whereas the sham animals exhibited higher ipsilateral withdrawal frequencies at 1 week only. There was no significant difference between NP-treatment and sham animals for the ipsilateral limb withdrawal frequency to the 2g von Frey filament ( $p = 0.20$ ), with both groups remaining within the range observed during preoperative evaluation.

In the contralateral limb, no significant differences between NP-treatment and sham animals were observed for either the 2g or 10g von Frey filament ( $p = 0.14$ ). However, the observed deviations from mean pre-operative withdrawal frequencies was opposite between treatment groups. Contralateral limb withdrawal frequency in the NP-treatment group at one week post-operatively was at the lower end of the preoperative range for the 10g filament, returning to normal at later time points after surgery. Among sham animals, contralateral limb withdrawal frequency was at the higher range of preoperative levels at one week post-operatively for the 10g filament, again returning to normal range of values at later time points.

While both groups exhibited greater thermal sensitivity following surgery, differences between NP-treated and sham animals were not observed in paw or tail withdrawal latency to thermal stimuli (data not shown).

### Gait Abnormalities

After surgery, both sham and NP-treatment animals ambulated with similar velocities ( $p = 0.35$ ), in the range of pre-operative observations (Figure 2, top panel). The gaits of NP-treated animals

had measures of asymmetry with values significantly higher than those observed in sham animals (Figure 2, middle panel,  $p < 0.05$ ), with the magnitude of these differences decreasing with time ( $p < 0.01$ ). At one week after surgery, a majority of NP-treated animals had gait symmetry above 0.5, suggesting inconsistent spacing in time between left and right foot-strikes manifested visually as a limp. NP-treatment animals also exhibited DF imbalances between left and right feet ( $\Delta DF \neq 0$ ), with no such observation for sham animals (Figure 2, bottom panel,  $p < 0.001$ ). The magnitude of these differences again decreased with time ( $p < 0.001$ ). At one and two weeks after surgery, the majority of NP-treated animals had gaits with  $\Delta DF$ s greater than 0, indicating more time spent on the limb contralateral to surgical intervention. These differences are again indicative of a limp. While NP-treatment animals tended to use wider step widths, no statistical differences between treatment groups were observed in step width ( $p = 0.09$ ), stride length ( $p = 0.79$ ), or stride frequency ( $p = 0.31$ ).

### Serum Cytokine Levels

Serum levels of all evaluated cytokines are shown as a function of treatment group and sacrifice time point in Table 1. Systemic expression of the tested cytokines did not differ significantly between sham and NP-treatment animals at any of the four time points studied (MANOVA, Wilk's lambda criteria,  $\alpha = 0.05$ ).

### Inflammatory and Immune Activation in the Dorsal Root Ganglion

Figure 3 provides representative examples of IL-17 and IL-23 staining illustrating ganglion, satellite, and Schwann cell expression in sham and NP-treatment animals. Substantial interobserver reliability was observed for all samples (quadratic-weighted Kappa of 0.74). Inflammatory activation measured by IL-23 immunoreactivity was equivalent between sham and NP-treatment for all cell types and time points (Student's t-test,  $\alpha = 0.05$ ). Conversely, early heightened IL-17 expression representative of immune activation was observed in NP-treatment animals compared to sham animals for ganglion cells (1 and 2 weeks), satellite cells (1 week), and Schwann cells (1 week) (Student's t-test,  $\alpha = 0.05$ ), with trends of higher expression at later time points. Mean immunohistochemical scores are tabulated in Table 2.

### Discussion

This animal model of radiculopathy was placing autologous tail NP onto an exposed lumbar DRG in treated animals, and comparing to animals undergoing simple surgical exposure alone. The technique of using tail NP ensures that the lumbar disc is neither injured by annular puncture nor weakened by NP evacuation. This helps in evaluating inflammatory and immune changes at the DRG specific to the presence of autologous NP, especially when annular incision alone can cause radiculopathy in animal models.<sup>36,37</sup>

A novel limping phenotype was observed in NP-treated animals shortly following surgery, characterized by changes in gait symmetry and onset of duty factor imbalance loading the contralateral limb. These biomechanical changes resolved four weeks after surgery and paralleled early heightened expression of autoimmune cytokines, suggesting potential resolution alongside elimination of the NP irritant. No changes in stride length or stride width were noted, consistent with findings by Olmarker and coworkers<sup>5</sup> in a similar model. Our quantitative findings of stride length and width agree with their results, but our novel addition of temporal variables of symmetry and duty factor proved valuable to characterize disability and potentially next evaluate benefit of therapeutic intervention. Further information about weight-bearing behavior after induced radiculopathy could be obtained using an incapacitance meter or by measuring gait dynamics by force plate.



Mechanical allodynia was observed in NP-treated animals (Figure 1, upper left panel), but a novel sensitivity pattern in the sham animal was also observed (Figure 1, upper right panel). Increased sensitivity in both ipsilateral and contralateral limbs among sham animals occurred at postoperative week one, interpreted as post-surgical sensitivity. This did not occur for the contralateral limb of NP-treated animals, for which there was decreased sensitivity in the first week compared to both sham animals and preoperative testing. This decrease may be attributed to heightened sensitivity of the ipsilateral limb of the NP-treated animal, now reluctant to load the contralateral limb despite mechanical stimulation. Further, the introduction of gait analysis into this study reveals a functional ambulatory consequence to this sensitivity, with asymmetric gait and decreased ipsilateral limb support most prominent at 1 week and still persistent at 2 weeks, with resolution at later time points (Figure 2, lower panel). Contrary to the stated heightened mechanical sensitivity, no change in withdrawal latency to thermal stimulus was observed in experimental versus sham animals. The absence of thermal hyperalgesia in combination with the mechanical allodynia has been previously observed in models of inflammatory neuritis utilizing either zymosan or TNF $\alpha$  as the stimulus. Further, intradermal delivery of capsaicin to humans creates a significantly larger field of mechanical than thermal sensitivity, suggesting the two to be mediated by alternate mechanisms – hyperalgesia peripherally by receptor sensitization and allodynia more centrally. Nevertheless, such dissociation of the two sensory modalities is likely to depend on the specific inflammatory stimulus, the additional induction of an immune response, and the presence of mechanical nerve root deformation.

Local DRG expression of IL-23 and IL-17 was examined at animal sacrifice with findings of equivalent IL-23 expression between the NP-treated and sham groups at all time points. This finding suggests that similar constitutive or surgically-stimulated release occurs in both groups, independent of NP placement on exposed neural structures. Of significance is early heightened expression of IL-17 in the NP-treatment group, suggesting additional autoimmune activation upon NP exposure, beyond the impact of surgical trauma. Requisite for such immune activation are an inflammatory stimulus with monocyte elaboration of IL-23, the presence of a T-lymphocyte of appropriate target specificity, and a target perceived as non-self. Taken together, the immunohistochemical results suggest that autoimmune reactivity against autologous NP may heighten DRG inflammation compared with animals undergoing sham surgery. The immune-privilege of this tissue potentiates autoimmune reactivity with radiculopathy symptoms upon systemic exposure following herniation. A proposed molecular mechanism for this immune privilege involves NP expression of the Fas ligand, causing apoptosis of invading Fas-positive T-cells.<sup>38</sup> Expression of this ligand decreases in the degenerating disc,<sup>39</sup> suggesting that herniation may both anatomically and biochemically activates the specific immune response. A caution when interpreting these results is that IL-17 staining was expressed at higher levels among NP-treated animals than controls for all cell types. As a small and freely-diffusible molecule, cytokine localization to the cell source of the cytokine is not definitive by immunohistochemistry alone, and several authors have suggested that astrocyte and oligodendrocyte IL-17 positivity may result from their scavenger cell activity.<sup>40,41</sup> Our results further demonstrate this finding in the peripheral nervous system counterparts of satellite cells and Schwann cells.

Local immune-mediated findings were not paralleled by increases in systemic cytokine expression. Equivalent levels between NP-treated and control groups supports previous clinical and experimental work revealing that the pathophysiology of disc-herniation radiculopathy is primarily mediated by local inflammation.<sup>42,43</sup> The trends toward decreasing TNF $\alpha$  expression across time reflects post surgical changes, but no difference was observed between study and control groups.

In conclusion, placement of autologous NP to overlies a lumbar DRG generated gait asymmetry and duty factor imbalance away from the affected limb. Mechanical allodynia persisted for the longitudinal duration of the study, with a sensitivity pattern coincident with the functional gait deficits. These findings identify useful parameters to evaluate potential therapeutic interventions in such disease models. The NP-treated and sham animals exhibited equivalent local inflammatory responses, but heightened expression of the autoimmune cytokine, IL-17, was observed primarily in animals exposed to autologous NP. These findings identify a new target pathway in the treatment of radiculopathy, with new functional parameters to evaluate their efficacy.

## Acknowledgements

The authors would like to thank Ms. Charlene Flahiff and Mr. Stephen Johnson for their assistance with the surgical procedures.

Funding Support: This work was supported with funds from Zimmer Orthopedics, the NIH (AR047442 and AR052745) and a Pratt-Gardner Predoctoral Research Fellowship.

## References

1. Winkelstein BA, Weinstein JN, DeLeo JA. The role of mechanical deformation in lumbar radiculopathy: an in vivo model. *Spine* 2002;27:27–33. [PubMed: 11805632]
2. Olmarker K, Storkson R, Berge OG. Pathogenesis of sciatic pain: a study of spontaneous behavior in rats exposed to experimental disc herniation. *Spine* 2002;27:1312–1317. [PubMed: 12065980]
3. Igarashi T, Kikuchi S, Shubayev V, et al. 2000 Volvo Award winner in basic science studies: Exogenous tumor necrosis factor-alpha mimics nucleus pulposus-induced neuropathology. Molecular, histologic, and behavioral comparisons in rats. *Spine* 2000;25:2975–2980. [PubMed: 11145807]
4. Kallakuri S, Takebayashi T, Ozaktay AC, et al. The effects of epidural application of allografted nucleus pulposus in rats on cytokine expression, limb withdrawal and nerve root discharge. *Eur Spine J* 2005;14:956–964. [PubMed: 15290408]
5. Olmarker K, Iwabuchi M, Larsson K, et al. Walking analysis of rats subjected to experimental disc herniation. *Eur Spine J* 1998;7:394–399. [PubMed: 9840473]
6. Otani K, Arai I, Mao GP, et al. Nucleus pulposus-induced nerve root injury: relationship between blood flow and motor nerve conduction velocity. *Neurosurgery* 1999;45:614–619. [PubMed: 10493381] discussion 9–20
7. Murata Y, Nannmark U, Rydevik B, et al. Nucleus pulposus-induced apoptosis in dorsal root ganglion following experimental disc herniation in rats. *Spine* 2006;31:382–390. [PubMed: 16481947]
8. Olmarker K, Nordborg C, Larsson K, et al. Ultrastructural changes in spinal nerve roots induced by autologous nucleus pulposus. *Spine* 1996;21:411–414. [PubMed: 8658242]
9. Murata Y, Onda A, Rydevik B, et al. Distribution and appearance of tumor necrosis factor-alpha in the dorsal root ganglion exposed to experimental disc herniation in rats. *Spine* 2004;29:2235–2241. [PubMed: 15480134]
10. Takahashi N, Kikuchi S, Shubayev VI, et al. TNF-alpha and phosphorylation of ERK in DRG and spinal cord: insights into mechanisms of sciatica. *Spine* 2006;31:523–529. [PubMed: 16508545]
11. Aoki Y, Rydevik B, Kikuchi S, et al. Local application of disc-related cytokines on spinal nerve roots. *Spine* 2002;27:1614–1617. [PubMed: 12163720]
12. Weiler C, Nerlich AG, Bachmeier BE, et al. Expression and distribution of tumor necrosis factor alpha in human lumbar intervertebral discs: a study in surgical specimen and autopsy controls. *Spine* 2005;30:44–53. [PubMed: 15626980]discussion 4
13. Le Maitre CL, Hoyland JA, Freemont AJ. Catabolic cytokine expression in degenerate and herniated human intervertebral discs: IL-1beta and TNFalpha expression profile. *Arthritis Res Ther* 2007;9:R77. [PubMed: 17688691]

14. Murata Y, Olmarker K, Takahashi I, et al. Effects of selective tumor necrosis factor-alpha inhibition to pain-behavioral changes caused by nucleus pulposus-induced damage to the spinal nerve in rats. *Neurosci Lett* 2005;382:148–152. [PubMed: 15911139]
15. Murata Y, Onda A, Rydevik B, et al. Selective inhibition of tumor necrosis factor-alpha prevents nucleus pulposus-induced histologic changes in the dorsal root ganglion. *Spine* 2004;29:2477–2484. [PubMed: 15543058]
16. Olmarker K, Rydevik B. Selective inhibition of tumor necrosis factor-alpha prevents nucleus pulposus-induced thrombus formation, intraneural edema, and reduction of nerve conduction velocity: possible implications for future pharmacologic treatment strategies of sciatica. *Spine* 2001;26:863–869. [PubMed: 11317106]
17. Onda A, Yabuki S, Kikuchi S. Effects of neutralizing antibodies to tumor necrosis factor-alpha on nucleus pulposus-induced abnormal nociceptive responses in rat dorsal horn neurons. *Spine* 2003;28:967–972. [PubMed: 12768133]
18. Genevay S, Stingelin S, Gabay C. Efficacy of etanercept in the treatment of acute, severe sciatica: a pilot study. *Ann Rheum Dis* 2004;63:1120–1123. [PubMed: 15115710]
19. Lee SJ, Han TR, Hyun JK, et al. Electromyographic findings in nucleus pulposus-induced radiculopathy in the rat. *Spine* 2006;31:2053–2058. [PubMed: 16915088]
20. Morag E, Hurwitz DE, Andriacchi TP, et al. Abnormalities in muscle function during gait in relation to the level of lumbar disc herniation. *Spine* 2000;25:829–833. [PubMed: 10751294]
21. Kawaguchi S, Yamashita T, Yokogushi K, et al. Immunophenotypic analysis of the inflammatory infiltrates in herniated intervertebral discs. *Spine* 2001;26:1209–1214. [PubMed: 11389385]
22. Murata Y, Rydevik B, Takahashi K, et al. Macrophage appearance in the epineurium and endoneurium of dorsal root ganglion exposed to nucleus pulposus. *J Peripher Nerv Syst* 2004;9:158–164. [PubMed: 15363063]
23. Bobechko WP, Hirsch C. Auto-Immune Response to Nucleus Pulposus in the Rabbit. *J Bone Joint Surg Br* 1965;47:574–580. [PubMed: 14341081]
24. Kanerva A, Kommonen B, Gronblad M, et al. Inflammatory cells in experimental intervertebral disc injury. *Spine* 1997;22:2711–2715. [PubMed: 9431603]
25. Habtemariam A, Gronblad M, Virri J, et al. Immunocytochemical localization of immunoglobulins in disc herniations. *Spine* 1996;21:1864–1869. [PubMed: 8875717]
26. Kawanokuchi J, Shimizu K, Nitta A, et al. Production and functions of IL-17 in microglia. *J Neuroimmunol* 2008;194:54–61. [PubMed: 18164424]
27. Kleinschnitz C, Hofstetter HH, Meuth SG, et al. T cell infiltration after chronic constriction injury of mouse sciatic nerve is associated with interleukin-17 expression. *Exp Neurol* 2006;200:480–485. [PubMed: 16674943]
28. Aggarwal S, Ghilardi N, Xie MH, et al. Interleukin-23 promotes a distinct CD4 T cell activation state characterized by the production of interleukin-17. *J Biol Chem* 2003;278:1910–1914. [PubMed: 12417590]
29. Langrish CL, Chen Y, Blumenschein WM, et al. IL-23 drives a pathogenic T cell population that induces autoimmune inflammation. *J Exp Med* 2005;201:233–240. [PubMed: 15657292]
30. Constantinescu CS, Tani M, Ransohoff RM, et al. Astrocytes as antigen-presenting cells: expression of IL-12/IL-23. *J Neurochem* 2005;95:331–340. [PubMed: 16086689]
31. Miljkovic D, Momcilovic M, Stojanovic I, et al. Astrocytes stimulate interleukin-17 and interferon-gamma production in vitro. *J Neurosci Res* 2007;85:3598–3606. [PubMed: 17969033]
32. Kebir H, Kreymborg K, Ifergan I, et al. Human TH17 lymphocytes promote blood-brain barrier disruption and central nervous system inflammation. *Nat Med* 2007;13:1173–1175. [PubMed: 17828272]
33. Kawakami M, Weinstein JN, Chatani K, et al. Experimental lumbar radiculopathy. Behavioral and histologic changes in a model of radicular pain after spinal nerve root irritation with chronic gut ligatures in the rat. *Spine* 1994;19:1795–1802. [PubMed: 7973977]
34. Olmarker K, Rydevik B, Nordborg C. Autologous nucleus pulposus induces neurophysiologic and histologic changes in porcine cauda equina nerve roots. *Spine* 1993;18:1425–1432. [PubMed: 8235812]



35. Hargreaves K, Dubner R, Brown F, et al. A new and sensitive method for measuring thermal nociception in cutaneous hyperalgesia. *Pain* 1988;32:77–88. [PubMed: 3340425]
36. Kayama S, Konno S, Olmarker K, et al. Incision of the anulus fibrosus induces nerve root morphologic, vascular, and functional changes. An experimental study. *Spine* 1996;21:2539–2543. [PubMed: 8961440]
37. Ulrich JA, Liebenberg EC, Thuillier DU, et al. ISSLS prize winner: repeated disc injury causes persistent inflammation. *Spine* 2007;32:2812–2819. [PubMed: 18246002]
38. Takada T, Nishida K, Doita M, et al. Fas ligand exists on intervertebral disc cells: a potential molecular mechanism for immune privilege of the disc. *Spine* 2002;27:1526–1530. [PubMed: 12131712]
39. Kaneyama S, Nishida K, Takada T, et al. Fas ligand expression on human nucleus pulposus cells decreases with disc degeneration processes. *J Orthop Sci* 2008;13:130–135. [PubMed: 18392917]
40. Tzartos JS, Friese MA, Craner MJ, et al. Interleukin-17 production in central nervous system-infiltrating T cells and glial cells is associated with active disease in multiple sclerosis. *Am J Pathol* 2008;172:146–155. [PubMed: 18156204]
41. Farina C, Aloisi F, Meinl E. Astrocytes are active players in cerebral innate immunity. *Trends Immunol* 2007;28:138–145. [PubMed: 17276138]
42. Brisby H, Olmarker K, Larsson K, et al. Proinflammatory cytokines in cerebrospinal fluid and serum in patients with disc herniation and sciatica. *Eur Spine J* 2002;11:62–66. [PubMed: 11931066]
43. Scuderi GJ, Brusovanik GV, Anderson DG, et al. Cytokine assay of the epidural space lavage in patients with lumbar intervertebral disk herniation and radiculopathy. *J Spinal Disord Tech* 2006;19:266–269. [PubMed: 16778661]

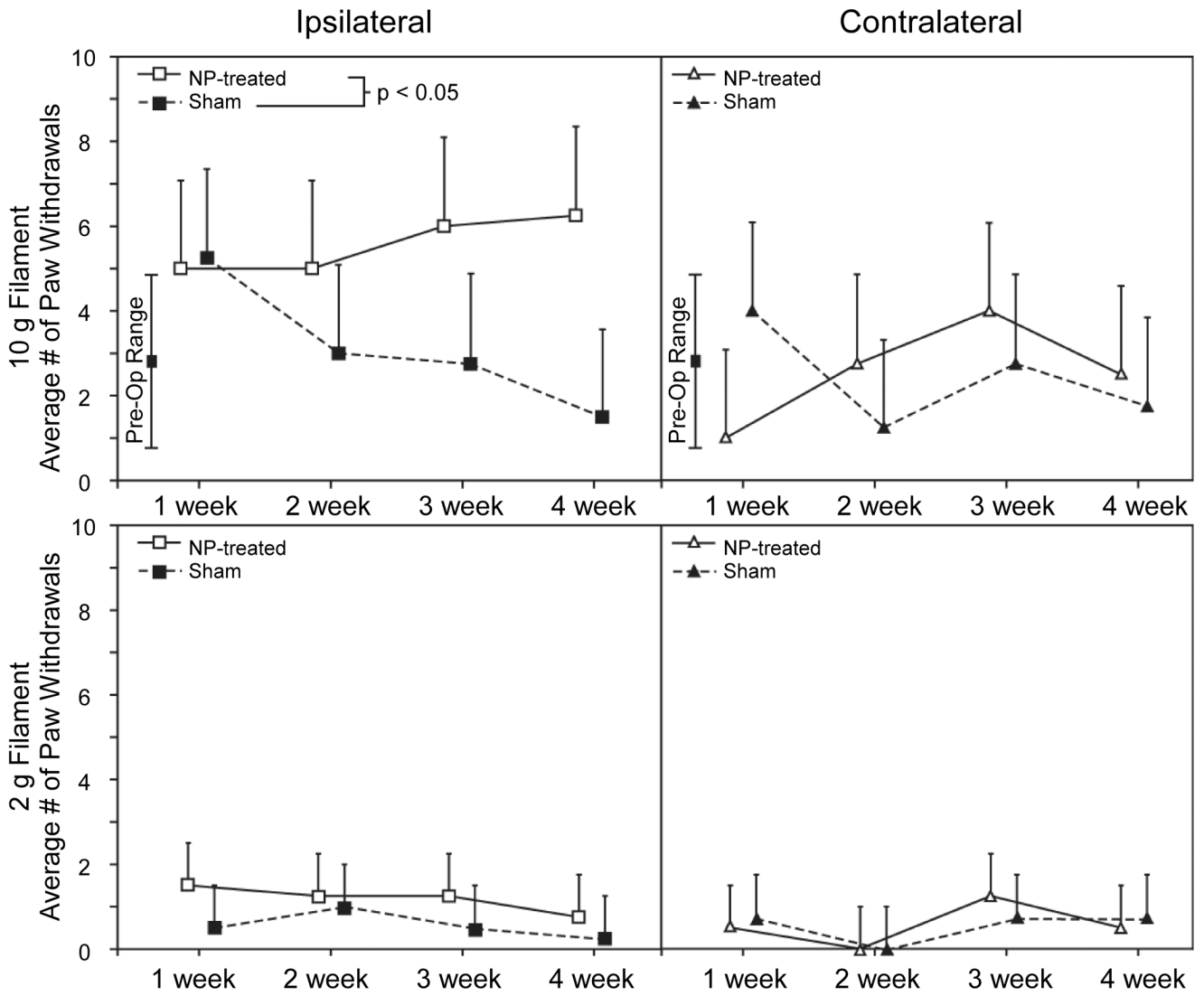


**Figure 1.** Mechanical sensitivity of the hindpaw ipsilateral (left panels) and contralateral (right panels) to DRG exposure are shown as the number of paw withdrawals per 10 applications of a 10 g (top panels) and 2 g (bottom panels) von Frey filament. Data are presented as mean + standard deviation for n = 4 animals per group. Response analysis via a generalized linear model revealed a prominent heightened ipsilateral limb sensitivity to the 10 g test in the NP-treated group relative to sham controls ( $p < 0.05$ ). Note the trend toward decreased mechanical sensitivity in the contralateral limb of NP-treated animals compared with the sham animals at 1 week, though this resolved at subsequent time points.

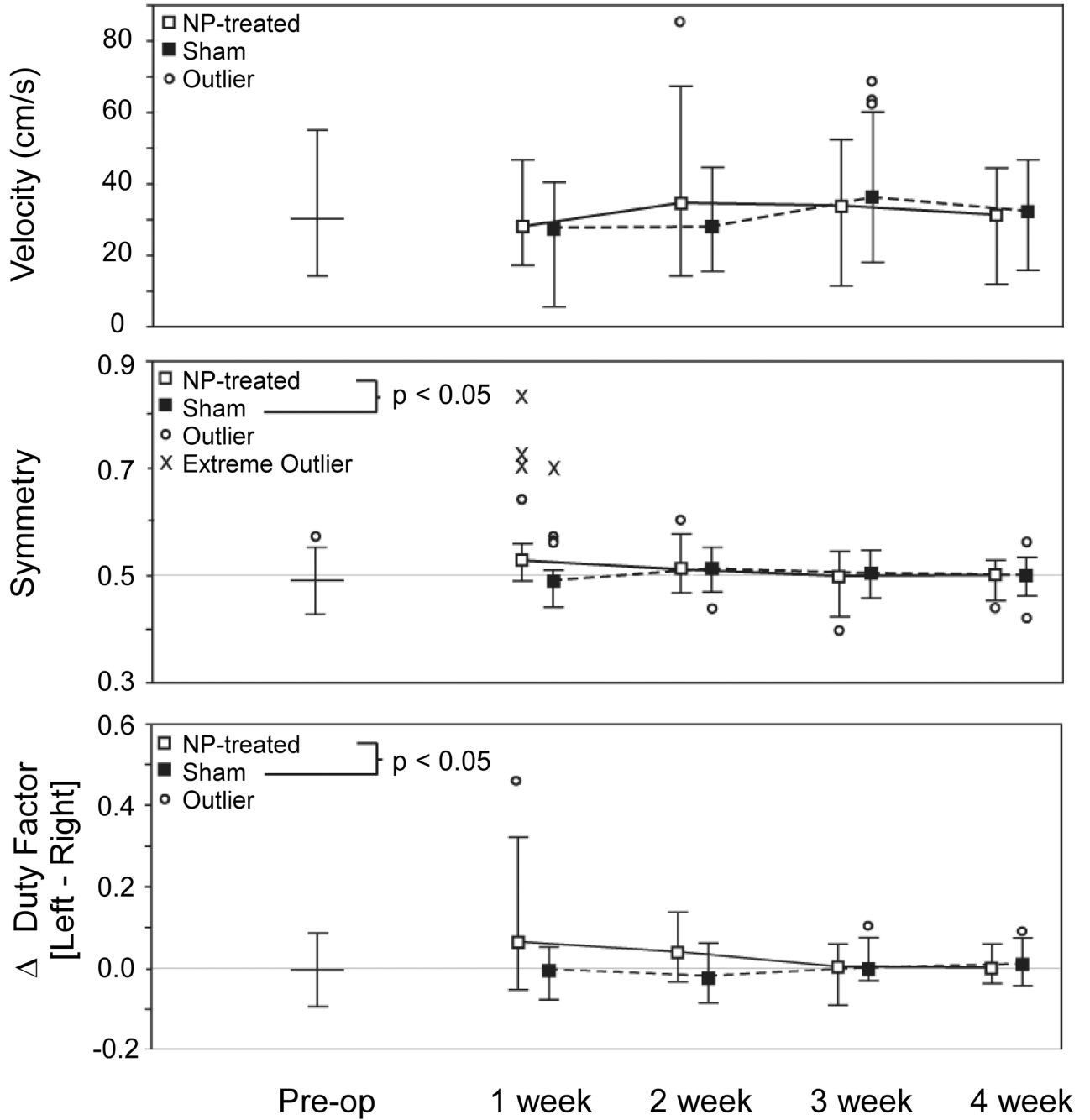


**Figure 2.** Analysis of gait parameters are shown for velocity (upper panel), symmetry (middle panel), and  $\Delta$  duty factor (lower panel). Data for NP-treated animals (white) and sham animals (black) are presented as median whisker plots of the non-outlier range for 4 animals per group with 4 and 7 successful trials per animal. No difference between treatment groups was observed for animal velocity ( $p = 0.35$ ). Animals in the NP-treated group had early gait asymmetry compared to sham animals ( $p < 0.05$ ), with the magnitude decreasing over time ( $p < 0.01$ ). Animals in the NP-treated group also spent more time on their contralateral limb, especially at early time points, reflected in an imbalance in duty factor ( $\Delta$ DF,  $p < 0.001$ ). These differences also decreased in magnitude over time ( $p < 0.001$ ).

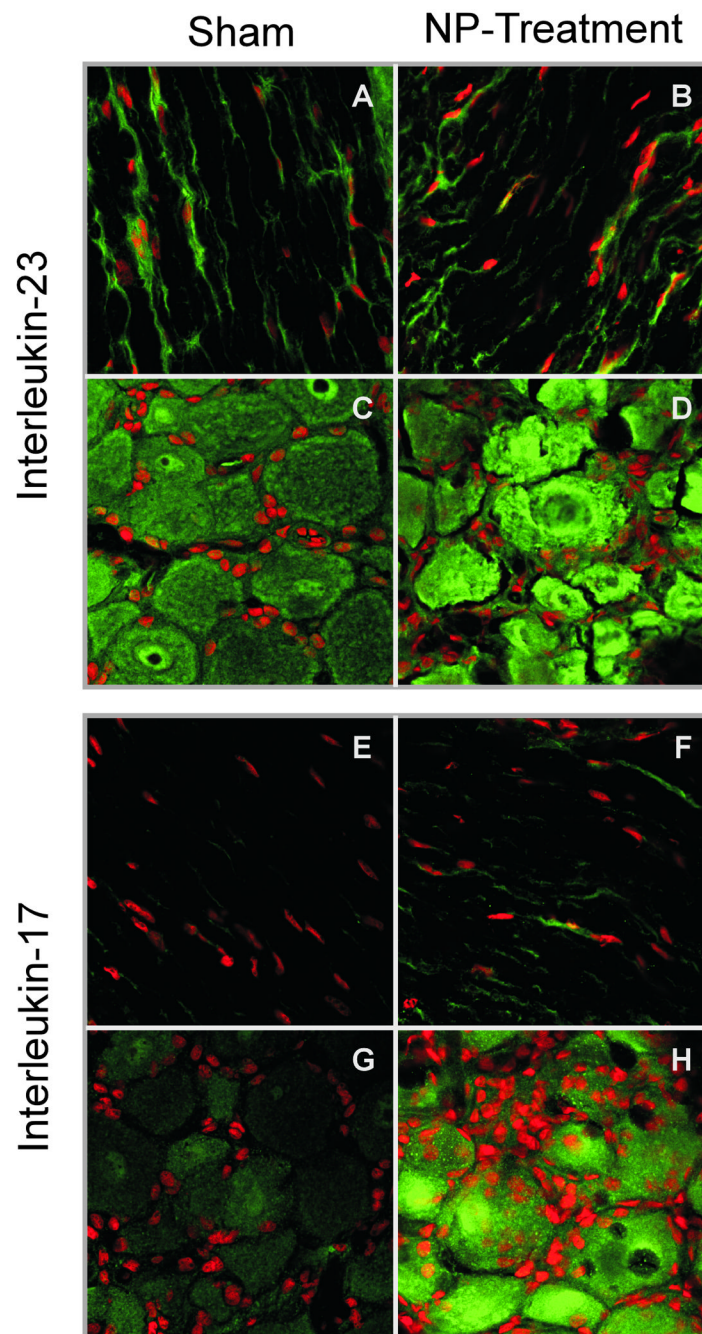


**Figure 3.** Examples of characteristic IHC slides demonstrating positivity for IL-23 (upper panels) and IL-17 (lower panels) in sham (left) and NP-treated (right). Panels A, B, E, and F are ganglion sections illustrating ganglion and satellite cells. Panels C, D, G, and H are axonal sections

**Table 1**  
Serum cytokine concentration stratified by time point and treatment

G:roup	IL-1 $\alpha$ pg/mL	IL-1 $\beta$ pg/mL	IL-4 pg/mL	IL-6 pg/mL	IL-12 pg/mL	GM- CSF pg/mL	IFN $\gamma$ pg/mL	TNF $\alpha$ pg/mL
<b>1 week</b>								
Sham	700 $\pm$ 300	60 $\pm$ 30	2.4 $\pm$ 0.2	13 $\pm$ 8	680 $\pm$ 110	80 $\pm$ 40	40 $\pm$ 20	440 $\pm$ 90
NP-treated	680 $\pm$ 110	50 $\pm$ 50	2.1 $\pm$ 0.3	17 $\pm$ 9	1000 $\pm$ 300	100 $\pm$ 30	60 $\pm$ 50	600 $\pm$ 300
<b>2 week</b>								
Sham	400 $\pm$ 200	20 $\pm$ 16	2.1 $\pm$ 0.3	6 $\pm$ 4	310 $\pm$ 140	80 $\pm$ 50	50 $\pm$ 30	180 $\pm$ 70
NP-treated	150 $\pm$ 60	130 $\pm$ 50	2.5 $\pm$ 0.4	6 $\pm$ 3	600 $\pm$ 400	60 $\pm$ 50	N/A	270 $\pm$ 140
<b>3 week</b>								
Sham	240 $\pm$ 100	100 $\pm$ 100	2.0 $\pm$ 0.2	9 $\pm$ 4	280 $\pm$ 120	23 $\pm$ 9	10 $\pm$ 5	100 $\pm$ 50
NP-treated	250 $\pm$ 110	30 $\pm$ 20	1.8 $\pm$ 0.2	9 $\pm$ 8	200 $\pm$ 110	16 $\pm$ 9	9 $\pm$ 4	200 $\pm$ 170
<b>4 week</b>								
Sham	400 $\pm$ 60	70 $\pm$ 40	2.2 $\pm$ 0.2	6 $\pm$ 5	670 $\pm$ 140	47 $\pm$ 14	18 $\pm$ 8	130 $\pm$ 40
NP-treated	330 $\pm$ 180	9 $\pm$ 5	1.9 $\pm$ 0.4	4 $\pm$ 2	340 $\pm$ 170	40 $\pm$ 30	30 $\pm$ 30	70 $\pm$ 30

Data are presented as mean  $\pm$  standard error. No significant differences were observed between sham and NP-treatment groups at the 0.05 level of significance.



**Table 2**  
Mean DRG immunohistochemical scores stratified by time point and treatment

Group	Ganglion		Satellite		Schwann	
	IL-17	IL-23	IL-17	IL-23	IL-17	IL-23
<b>1 week</b>						
Sham	1.1 ± 0.1	2.5 ± 0.5	0.2 ± 0.1	2.7 ± 0.3	0 ± 0	1 ± 0
NP-treated	<b>2.5 ± 0.2 *</b>	1.8 ± 0.5	<b>2.3 ± 0.3 *</b>	1.8 ± 0.4	<b>1.4 ± 0.3 *</b>	<b>2.7 ± 0.0 *</b>
<b>2 week</b>						
Sham	1.7 ± 0.4	2.3 ± 0.5	1.0 ± 0.3	2.3 ± 0.1	0.7 ± 0.2	2.1 ± 0.2
NP-treated	<b>2.9 ± 0.1 *</b>	2.9 ± 0.1	2.1 ± 0.6	1.9 ± 0.5	1.3 ± 0.2	<b>1.4 ± 0.1 *</b>
<b>3 week</b>						
Sham	1.1 ± 0.1	1.4 ± 0.1	0.4 ± 0.3	2.3 ± 0.3	0 ± 0	2.8 ± 0.2
NP-treated	1.8 ± 0.7	1.8 ± 0.7	1.0 ± 0.7	2.4 ± 0.3	0.8 ± 0.3	2.3 ± 0.3
<b>4 week</b>						
Sham	1.2 ± 0.1	2.3 ± 0.3	0.7 ± 0.2	2.2 ± 0.1	1.2 ± 0.2	2.0 ± 0.5
NP-treated	2.3 ± 0.4	2.3 ± 0.4	1.2 ± 0.4	2.0 ± 0.4	1.0 ± 0.1	1.9 ± 0.3

Data are presented as mean ± standard error.

\* denotes significant difference by Student's t-test of the NP-treatment from the sham group at the 0.05 level of significance.